Cavity-Containing [Fe₂L₃]⁴⁺ Helicates: An Examination of Host-Guest Chemistry and Cytotoxicity

Lynn S. Lisboa[1†], Mie Riisom[2,3†], Roan A. S. Vasdev[1†], Stephen M. F. Jamieson[3†], L. James Wright[2†], Christian G. Hartinger[2†] and James D. Crowley[1*†]
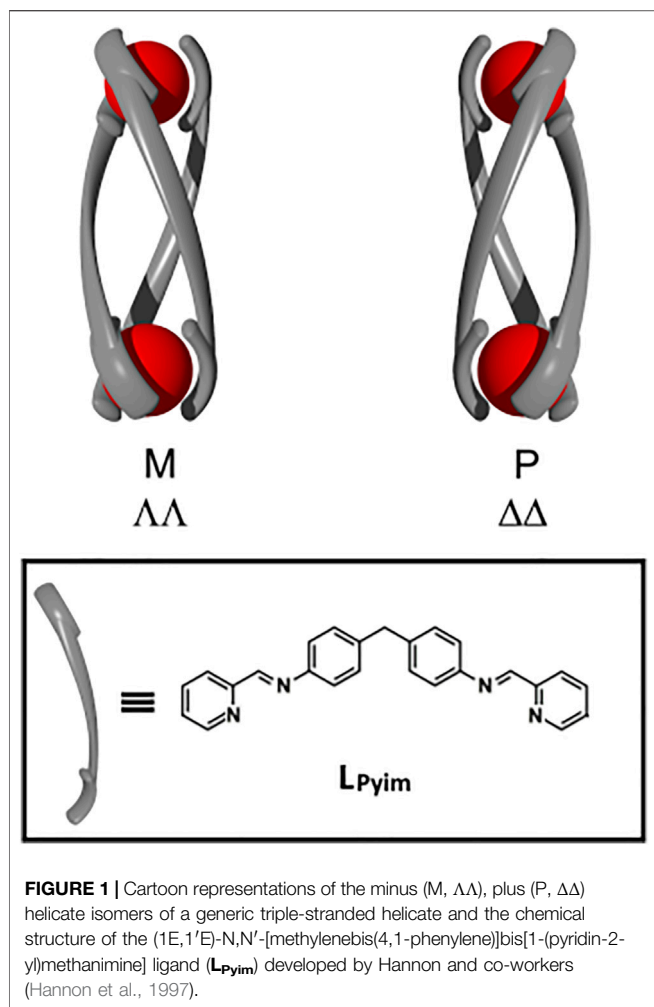
[1]Department of Chemistry, University of Otago, Dunedin, New Zealand, [2]School of Chemical Sciences, University of Auckland, Auckland, New Zealand, [3]Auckland Cancer Society Research Centre, University of Auckland, Auckland, New Zealand

Two new di(2,2′-bipyridine) ligands, 2,6-bis([2,2′-bipyridin]-5-ylethynyl)pyridine (**L1**) and bis(4-([2,2′-bipyridin]-5-ylethynyl)phenyl)methane (**L2**) were synthesized and used to generate two metallosupramolecular [Fe₂(**L**)₃](BF₄)₄ cylinders. The ligands and cylinders were characterized using elemental analysis, electrospray ionization mass spectrometry, UV-vis, ¹H-, ¹³C and DOSY nuclear magnetic resonance (NMR) spectroscopies. The molecular structures of the [Fe₂(**L**)₃](BF₄)₄ cylinders were confirmed using X-ray crystallography. Both the [Fe₂(**L1**)₃](BF₄)₄ and [Fe₂(**L2**)₃](BF₄)₄ complexes crystallized as racemic (*rac*) mixtures of the ΔΔ (P) and ΛΛ (M) helicates. However, ¹H NMR spectra showed that in solution the larger [Fe₂(**L2**)₃](BF₄)₄ was a mixture of the *rac*-ΔΔ/ΛΛ and *meso*-ΔΛ isomers. The host-guest chemistry of the helicates, which both feature a central cavity, was examined with several small drug molecules. However, none of the potential guests were found to bind within the helicates. *In vitro* cytotoxicity assays demonstrated that both helicates were active against four cancer cell lines. The smaller [Fe₂(**L1**)₃](BF₄)₄ system displayed low μM activity against the HCT116 (IC₅₀ = 7.1 ± 0.5 μM) and NCI-H460 (IC₅₀ = 4.9 ± 0.4 μM) cancer cells. While the antiproliferative effects against all the cell lines examined were less than the well-known anticancer drug cisplatin, their modes of action would be expected to be very different.

Keywords: iron(II), helicate, cytotoxicity, host-guest chemistry, metallosupramolecular architectures

INTRODUCTION

Metallosupramolecular architectures (MSAs) are beginning to display a wide range of applications (Yoshizawa et al., 2009; Cook and Stang, 2015; Hong et al., 2018; Saha et al., 2018; Bardhan and Chand, 2019; Gao et al., 2019; Rizzuto et al., 2019; Percastegui et al., 2020) Largely inspired by the success of small molecule metallo-drugs (Hartinger and Dyson, 2009; Mjos and Orvig, 2014; Anthony et al., 2020; Boros et al., 2020; Frei, 2020; Frei et al., 2020; Steel et al., 2021b) there is a growing interest in biological applications of MSAs (Cook et al., 2013; Therrien, 2015; Pöthig and Casini, 2019; Sepehrpour et al., 2019; Samanta and Isaacs, 2020). Systems have been studied for their anti-cancer and anti-microbial activity and their potential as drug delivery agents. Helicates (Piguet et al., 1997; Albrecht, 2001; Hannon and Childs, 2004; Howson and Scott, 2011; Boiocchi and Fabbrizzi, 2014; Paneerselvam et al., 2018; Albrecht et al., 2019; Albrecht, 2020; Tran and Yoo, 2020) are one of the earlier known and well-studied sub-classes of MSAs. Lehn and co-workers reported the first helicates; a double-stranded dinuclear and larger trinuclear system were generated from poly(2,2′-bipyridine)

FIGURE 1 | Cartoon representations of the minus (M, ΛΛ), plus (P, ΔΔ) helicate isomers of a generic triple-stranded helicate and the chemical structure of the (1E,1′E)-N,N′-[methylenebis(4,1-phenylene)]bis[1-(pyridin-2-yl)methanimine] ligand (**L$_{Pyim}$**) developed by Hannon and co-workers (Hannon et al., 1997).

octahedral metal ion and di(bidentate) linker ligands [M₂L₃]; this combination of building blocks can generate three isomeric complexes the chiral M (ΛΛ) and P (ΔΔ), and the *meso* (ΛΔ). Pioneering work by Hannon and co-workers described the synthesis of the first [Fe₂(**L$_{Pyim}$**)₃]⁴⁺ helicates (where **L$_{Pyim}$** = (1E,1′E)-N,N′-[methylenebis(4,1-phenylene)]bis[1-(pyridin-2-yl) methanimine], **Figure 1**] obtained from pyridylimine binding motifs, octahedral Fe(II) ions and a diphenylmethylene spacer unit (Hannon et al., 1997). The mechanical coupling exerted by the spacer unit meant that a racemic (*rac*) mixture of the M (ΛΛ) and P (ΔΔ) [M₂(**L$_{Pyim}$**)₃]⁴⁺ helicates (where M = Fe(II) or Ni(II)) was formed and the authors went on to show that the M and P helicates could be resolved by chiral chromatography (Hannon et al., 2001a). The interaction of the M– and P–[Fe₂(**L$_{Pyim}$**)₃]⁴⁺ helicates with DNA has been extensively examined. The complexes have been shown to bind in the major grove of duplex DNA (Moldrheim et al., 2002), and at the center of three-way DNA (Oleksi et al., 2006; Cerasino et al., 2007; Malina et al., 2007; Cardo et al., 2011) and RNA (Phongtongpasuk et al., 2013) junctions (3WJ). More recently, the [Fe₂(**L$_{Pyim}$**)₃]⁴⁺ helicates were also shown to bind to DNA and RNA bulges (Malina et al., 2014; Malina et al., 2016). Similar observations have been made with the related [M₂(**L$_{Pyim}$**)₃]⁴⁺ helicates [where M = Ru(II) or Ni(II)] (Cardo et al., 2018) and the Ni(II) and Fe(II) helicates have been demonstrated to interact with G-quadruplexes (Zhao et al., 2013; Zhao et al., 2016) and the β-amyloid polypeptide (Aβ) (Yu et al., 2012; Li et al., 2015). Furthermore, the interaction of the iron(II) helicate with duplex DNA induces intramolecular DNA coiling (Hannon et al., 2001b; Malina et al., 2008) and it has been shown to display anti-cancer (Hotze et al., 2008), anti-bacterial (Richards et al., 2009) and anti-fungal (Vellas et al., 2013) properties, but is not mutagenic or genotoxic. This remarkable range of biological properties has been obtained without investigating changes to either the metal binding (pyridylimine) or spacer units of the helicates, suggesting that the system could potentially be improved by further tuning of the molecular scaffold.

Building on the aforenoted work, Scott and co-workers developed an excellent method for the self-assembly of optically pure single diastereomer *fac*-[Fe(**L$_{pyimR}$**)₃]²⁺ (where **L$_{pyimR}$** = functionalized pyridylimine ligand) complexes (Howson et al., 2009). The same group then exploited this method to synthesize enantiomerically pure Fe(II) and Zn(II) [M₂(**L$_{pyimR}$**)₃]⁴⁺ helicates and flexicates which feature different spacer systems. Like the parent Hannon helicate, it has been shown that these new pyridylimine-based complexes have shown a diverse range of biological properties and some flexicates have impressive, tunable anti-microbial (Howson et al., 2012; Simpson et al., 2019) and anti-cancer (Brabec et al., 2013; Faulkner et al., 2014; Kaner and Scott, 2015; Kaner et al., 2016; Song et al., 2019; Song et al., 2020) properties. The interactions of this more diverse family of helicates with DNA/RNA (Song et al., 2021) and proteins (Li et al., 2014) have also been examined and the systems show structure-dependent binding to duplex DNA (Brabec et al., 2013; Malina et al., 2015b), G-quadruplexes (Zhao et al., 2017; Zhao et al., 2018), 3WJ and 4WJ (Brabec et al., 2013), and bulges (Malina et al., 2015a; Hrabina et al., 2020).
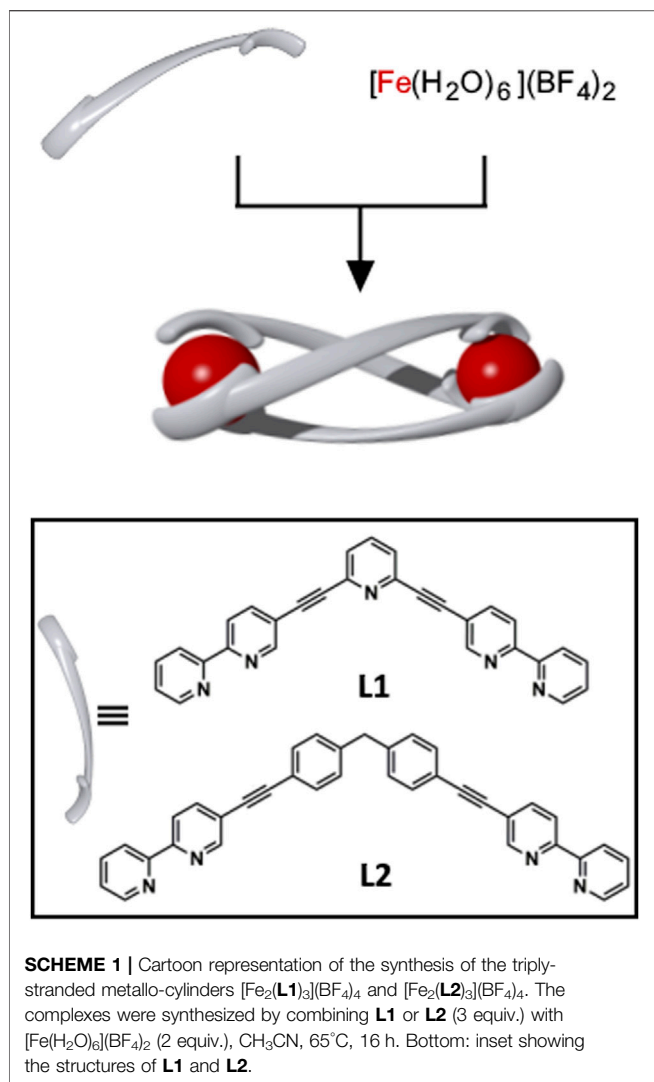
ligands and Cu(I) ions (Lehn et al., 1987) Subsequently, single, triple, and quadruple stranded helicates have all been synthesized and these systems are chiral featuring P (plus, right-handed) and M (minus, left-handed) helices (**Figure 1**). Because of the structural relationship to helical natural materials such as DNA, α-helices and zinc fingers of proteins there has been considerable interest in the biological properties, of helicates. Early work by Lehn and co-workers showed that double-stranded helicates assembled from poly(2,2′-bipyridine) ligands and Cu(I) ions could bind to double stranded DNA (Schoentjes and Lehn, 1995). Others have examined DNA binding and nuclease activity (Childs et al., 2006), and the cytotoxicity of related double-stranded complexes (Holtze et al., 2006; Allison et al., 2018). In addition, quadruple-stranded helicates have been shown to be cytotoxic (Mcneill et al., 2015; Ahmedova et al., 2016a; Ahmedova et al., 2016b; Schmidt et al., 2016; Vasdev et al., 2018; Ahmedova et al., 2020) and in some cases the modes of action of the complexes have been studied (Mcneill et al., 2020).

While there are only a few reports on the biological properties of double- and quadruple-stranded helicates, the related triple-stranded analogues have been extensively examined. These triply-stranded supramolecular structures are assembled from an

SCHEME 1 | Cartoon representation of the synthesis of the triply-stranded metallo-cylinders [Fe$_2$(**L1**)$_3$](BF$_4$)$_4$ and [Fe$_2$(**L2**)$_3$](BF$_4$)$_4$. The complexes were synthesized by combining **L1** or **L2** (3 equiv.) with [Fe(H$_2$O)$_6$](BF$_4$)$_2$ (2 equiv.), CH$_3$CN, 65°C, 16 h. Bottom: inset showing the structures of **L1** and **L2**.

The success of the pyridylimine [M$_2$L$_3$]$^{4+}$ helicates discussed above has inspired others to examine the biological properties of related [M$_2$L$_3$]$^{4+}$ triply-stranded helicates. For example, we have explored the use of small families of di(2-pyridyl-1,2,3-triazole) ligands (**L$_{dipytri}$**) to generate Fe(II), Ru(II), and Co(III) helicates (Vellas et al., 2013; Kumar et al., 2015; Vasdev et al., 2016). The biological properties of the Fe(II) and Ru(II) systems were poor but the more robust Co(III) helicates were shown to bind to and condense DNA and in addition displayed good anticancer activity (Crlikova et al., 2020). Di(2,2′-bipyridine) ligands (Glasson et al., 2008; Glasson et al., 2011a; Glasson et al., 2011b) have also been used to generate [M$_2$L$_3$]$^{4+}$ triple-stranded helicates and recently Vázquez and co-workers have examined the DNA binding and cytotoxicity of some peptide linked [M$_2$L$_3$]$^{4+}$ helicates [where M = Fe(II) or Co(III)] (Gamba et al., 2014; Gómez-González et al., 2018; Gomez-Gonzalez et al., 2021).

Given the well demonstrated ability of [M$_2$L$_3$]$^{4+}$ helicates to bind to DNA/RNA and proteins and their potential to be used as targeted therapeutics, we herein report the synthesis of two new

di(2,2′-bipyridine) ligands, 2,6-bis([2,2′-bipyridin]-5-ylethynyl)-pyridine (**L1**) and bis(4-([2,2′-bipyridin]-5-ylethynyl)phenyl)-methane (**L2**) and their use in the assembly of two new triple-stranded [Fe$_2$L$_3$]X$_4$ helicates (X = BF$_4^-$, OTf$^-$ or Cl$^-$). Moreover, due the presence of a central cavity in both the [Fe$_2$(**L1**)$_3$](BF$_4$)$_4$ and [Fe$_2$(**L2**)$_3$](BF$_4$)$_4$ helicates, we also report our examination of the host-guest properties of these systems with some small molecule drugs and our studies of the anti-cancer activity of the complexes.
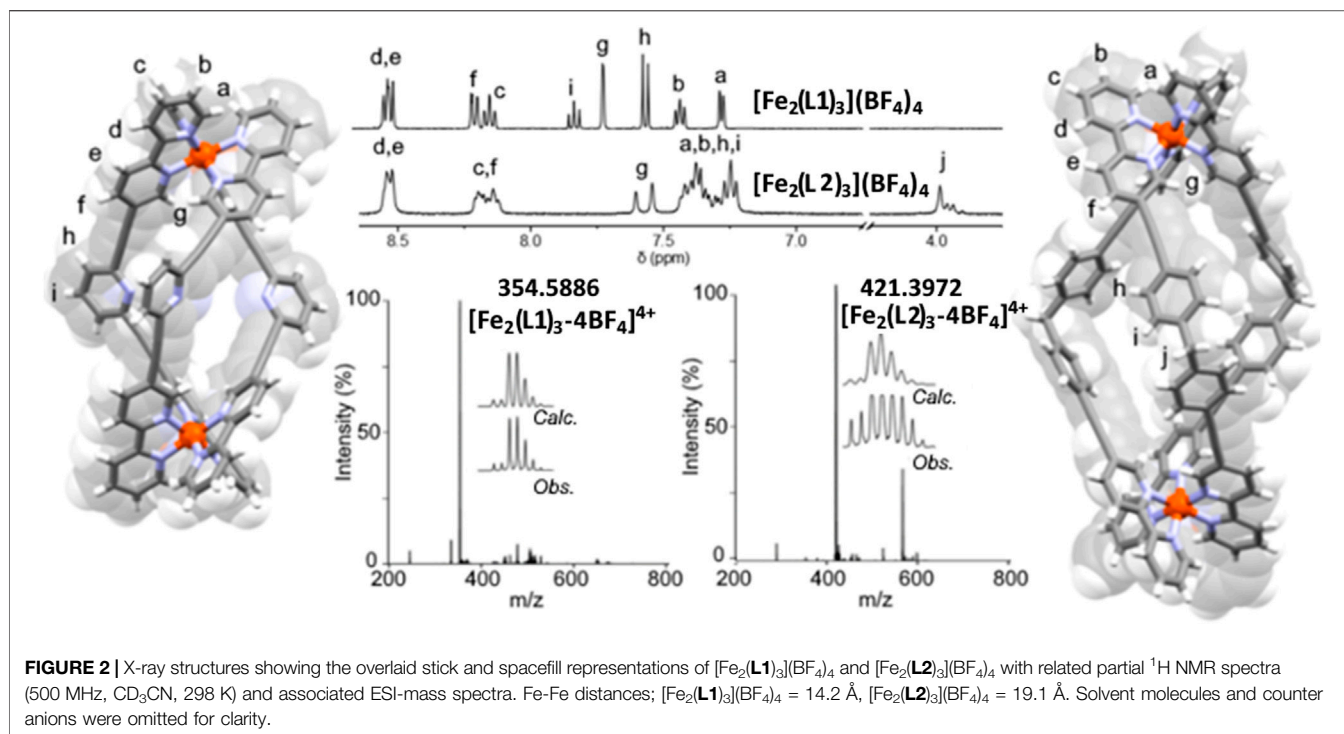
RESULTS AND DISCUSSION

The new di(2,2′-bipyridine) ligands, 2,6-bis([2,2′-bipyridin]-5-ylethynyl)-pyridine (**L1**) and bis(4-([2,2′-bipyridin]-5-ylethynyl)-phenyl)methane (**L2**) were synthesized from 5-ethynyl-2,2′-bipyridine (Grosshenny et al., 1997) and either 2,5-dibromopyridine or bis(4-iodophenyl)methane (Austin et al., 1981) using standard Sonogashira cross-coupling conditions (**Supplementary Material**) and were obtained in modest yields (**L1** = 51% and **L2** = 61%). The ligands were characterized using ^{1}H nuclear magnetic resonance (NMR), ^{13}C {^{1}H} NMR, electrospray ionization mass spectrometry (ESIMS) and elemental analysis (**Supplementary Figures S1–S4**).

The [Fe$_2$(**L**)$_3$](BF$_4$)$_4$ helicates were synthesised by combining either **L1** or **L2** (3 equiv.) with [Fe(H$_2$O)$_6$](BF$_4$)$_2$ (2 equiv.) in acetonitrile at 65°C (**Scheme 1** and **Supplementary Material**). The ligands were initially insoluble in the reaction mixture, however, after 5 min the ligands dissolved and deep red solutions (λ_{max} = 545 or 547 nm, respectively) were obtained. The resulting Fe(II) complexes were purified by recrystallization (vapour diffusion of diethyl ether into a nitromethane solution) and deep red crystals were isolated in good yields (89% for [Fe$_2$(**L1**)$_3$](BF$_4$)$_4$ and 77% for [Fe$_2$(**L2**)$_3$](BF$_4$)$_4$). The complexes were characterised by ^{1}H NMR, ^{13}C{^{1}H} NMR, ^{1}H DOSY NMR, UV-vis spectroscopy, ESIMS, and X-ray crystallography (**Supplementary Material**).

The ESIMS data obtained for the two complexes displayed a major peak consistent with the corresponding [Fe$_2$L$_3$]$^{4+}$ cation (m/z = 354.5886 [Fe$_2$(**L1**)$_3$]$^{4+}$ and m/z = 421.3972 m/z [Fe$_2$(**L2**)$_3$]$^{4+}$, respectively) suggestive of the formation of the expected triple-stranded helicates (Figure, **Supplementary Figures S7, S10**). The ^{1}H DOSY NMR spectra (500 MHz, CD$_3$CN, 298 K) of [Fe$_2$(**L1**)$_3$](BF$_4$)$_4$ and [Fe$_2$(**L2**)$_3$](BF$_4$)$_4$ were collected, and all the proton resonances displayed the same diffusion coefficients (6.51 ± 0.03 × 10^{-10} m^2 s^{-1} and 5.40 ± 0.10 × 10^{-10} m^2 s^{-1}, respectively) suggesting that a single metallosupramolecular architecture or mixtures of isomeric architectures were obtained (**Supplementary Figures S11, S12**). In addition, the observed diffusion coefficients were similar to those found for some related [Fe$_2$(**L$_{dipytri}$**)$_3$]$^{4+}$ metallo-cylinders (Vellas et al., 2013) providing further support for the formation of the desired triple-stranded helicates.

The ^{1}H NMR spectra (500 MHz, CD$_3$CN, 298 K) for the complexes of **L1** and **L2** were significantly distinct (**Figure 2**; **Supplementary Material**). The spectrum of [Fe$_2$(**L1**)$_3$](BF$_4$)$_4$ displayed nine sharp resonances in the

FIGURE 2 | X-ray structures showing the overlaid stick and spacefill representations of [Fe$_2$(**L1**)$_3$](BF$_4$)$_4$ and [Fe$_2$(**L2**)$_3$](BF$_4$)$_4$ with related partial ^{1}H NMR spectra (500 MHz, CD$_3$CN, 298 K) and associated ESI-mass spectra. Fe-Fe distances; [Fe$_2$(**L1**)$_3$](BF$_4$)$_4$ = 14.2 Å, [Fe$_2$(**L2**)$_3$](BF$_4$)$_4$ = 19.1 Å. Solvent molecules and counter anions were omitted for clarity.

aromatic region (δ = 8.5–7.0 ppm) consistent with the formation of a racemic (*rac*) mixture of the helical [Fe$_2$(**L1**)$_3$]$^{4+}$ isomers, P = $\Delta\Delta$ and M = $\Lambda\Lambda$. Conversely, the ^{1}H NMR spectrum of [Fe$_2$(**L2**)$_3$](BF$_4$)$_4$ was more complex with several broad overlapping resonances in the aromatic region. However, the methylene protons of the spacer backbone (H$_j$, δ = 4.0–3.8 ppm) were clearly split into two distinct resonances; a singlet and an AB quartet. This suggests that in solution [Fe$_2$(**L2**)$_3$](BF$_4$)$_4$ forms a mixture of helicate *rac*-$\Delta\Delta$/$\Lambda\Lambda$ and mesocate *meso*-$\Delta\Lambda$ isomers. Others (Goetz and Kruger, 2006; Vellas et al., 2013) have observed this behavior in solution with related [Fe$_2$L$_3$]$^{4+}$ systems that feature the diphenylmethylene spacer unit. This is in contrast to observations with the pyridyl imine helicate, [Fe$_2$(**L**$_{\text{Pyim}}$)$_3$]$^{4+}$ of Hannon and co-workers (Hannon et al., 1997). Those helicates have the same spacer unit and are found to exclusively form *rac*-helicates in solution and the solid state. The difference appears to be related to the larger size of [Fe$_2$(**L2**)$_3$]$^{4+}$ compared to [Fe$_2$(**L**$_{\text{Pyim}}$)$_3$]$^{4+}$. In [Fe$_2$(**L**$_{\text{Pyim}}$)$_3$]$^{4+}$, the aryl rings of the spacer unit are in close contact and interdigitate, mechanically locking the complex into the helical arrangement. The larger size of **L2** lessens this steric interdigitation of the spacer aryl groups, therefore making the mesocate arrangement more energetically accessible.

The molecular structures of [Fe$_2$(**L1**)$_3$](BF$_4$)$_4$ and [Fe$_2$(**L2**)$_3$](BF$_4$)$_4$ were confirmed by X-ray crystallography with crystals grown by slow vapour diffusion of diethyl ether into nitromethane solutions (**Figure 2**, **Supplementary Figures S27, S28**). The [Fe$_2$(**L1**)$_3$](BF$_4$)$_4$ structure was solved in the $P\bar{1}$ space group and the asymmetric unit contains two iron ions, three **L1** ligands, four tetrafluoroborate anions and two nitromethane solvent molecules. Each iron(II) ion is coordinated to three

bipy units generating a triple-stranded helicate architecture. The Fe-Fe distance of 14.2 Å confirmed that the system is elongated in comparison to the parent Hannon helicate. The compound crystallized as a racemic mixture in the solid state with both the $\Delta\Delta$ (P) and $\Lambda\Lambda$ (M) isomers (see the structural representations in **Figure 2**) present in the crystal.

The [Fe$_2$(**L2**)$_3$](BF$_4$)$_4$ structure was solved in the $P2_1/n$ space group and the asymmetric unit was occupied by one [Fe$_2$(**L2**)$_3$]$^{4+}$ unit, two tetrafluoroborate anions and seven co-crystallized nitromethane molecules. [Fe$_2$(**L2**)$_3$](BF$_4$)$_4$ was shown to crystallize as a *rac* mixture of the $\Delta\Delta$ (P) and $\Lambda\Lambda$ (M) helicates. The *meso*-form detected in solution by ^{1}H NMR spectroscopy was not observed in the solid state, presumably due to crystal packing effects (Vellas et al., 2013). The combination of the two 5-ethynyl-2,2′-bipyridine units and the diphenylmethylene spacer in **L2** led to a large Fe-Fe distance (19.1 Å) in [Fe$_2$(**L2**)$_3$](BF$_4$)$_4$. The metallo-architectures of both [Fe$_2$(**L1**)$_3$](BF$_4$)$_4$ and [Fe$_2$(**L2**)$_3$](BF$_4$)$_4$ displayed a clear central cavity and notable π surfaces available for potential host-guest interactions (**Figure 2**; **Supplementary Material**).

MSA cage systems have been used extensively as hosts for small molecule guests (Yoshizawa et al., 2009; Cook and Stang, 2015; Hong et al., 2018; Saha et al., 2018; Bardhan and Chand, 2019; Gao et al., 2019; Rizzuto et al., 2019; Percastegui et al., 2020). In contrast, the use of [Fe$_2$L$_3$]$^{4+}$ helicate architectures as hosts is far less common, presumably because the vast majority of reported MSAs do not contain a central cavity. Recently, there have been a few reports of guest binding [anions (Goetz and Kruger, 2006; Cui et al., 2012), sugars (Yang et al., 2021) and small aromatic molecules (Fazio et al., 2018; Jiang et al., 2019)] within [Fe$_2$L$_3$]$^{4+}$ helicates that feature small cavities. As the cavities of

FIGURE 3 | Guest molecules examined in the host-guest study with the helicates.
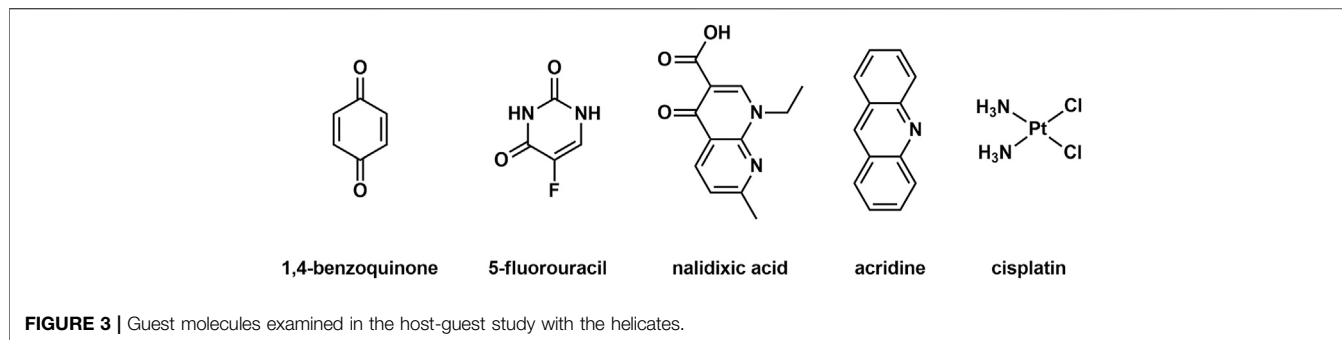
the $[Fe_2(\textbf{L1})_3]^{4+}$ and $[Fe_2(\textbf{L2})_3]^{4+}$ helicates are both lined by functional groups that could interact with guests through either hydrogen bonding or π-interactions, we sought out some small drug molecules that could potentially interact with the helicates using those non-covalent interactions. Therefore, the guest molecules 1,4-benzoquinone, nalidixic acid, acridine (as an analogue of proflavine), cisplatin and 5-fluorouracil were selected as they are either known or analogues of known anticancer and antibacterial drugs (**Figure 3**; **Supplementary Material**). The host-guest (HG) interactions were examined using ^{1}H NMR spectroscopy and ESIMS. One of the potential guest molecules (2 equiv.) was combined with one of the helicates (1 equiv.) in CD_3CN at 298 K and the ^{1}H NMR spectrum acquired (**Supplementary Material**). ^{1}H NMR spectra of the host-guest mixtures were then compared to the ^{1}H NMR spectra of the corresponding "free" host and guest compounds (**Supplementary Figures S23, S24**). Disappointingly, no complexation induced shifts were observed for either the host or the guest resonances suggesting that none of the guests bound within the cavities of the helicates. Molecular models (SPARTAN16, MMFF, **Supplementary Figures S25, S26**) showed that there are no obvious steric interactions that would prevent host-guest formation for the majority of the examined HG pairs. Thus, the lack of guest binding in the cases examined appears to be due to the absence of the correct combination of complementary non-covalent and solvaphobic interactions. Additionally, the BF_4^- counter-anions may be competing for the cavity as has been observed in other cationic MSA systems (August et al., 2016).

Related $[Fe_2L_3]^{4+}$ helicates have shown excellent anticancer activity (Song et al., 2021). Therefore, we examined the cytotoxicity of $[Fe_2(\textbf{L1})_3]^{4+}$ and $[Fe_2(\textbf{L2})_3]^{4+}$ against a panel of cancer cell lines. As the $[Fe_2(\textbf{L1})_3](BF_4)_4$ and $[Fe_2(\textbf{L2})_3](BF_4)_4$ complexes were only soluble in polar organic solvents (DMSO, CH_3CN, CH_3NO_2, and acetone) we attempted to render the helicates water soluble by exchanging the BF_4^- counter anions with Cl^- or OTf^- (**Supplementary Material**). While we were able to generate the new $[Fe_2(\textbf{L1})_3](X)_4$ and $[Fe_2(\textbf{L2})_3](X)_4$ (where X = Cl^-, OTf^-) salts, they proved even less soluble than the original BF_4^- salts. The OTf^- salts were soluble in CH_3CN and DMSO, however, the Cl^- salts were only soluble in DMSO with none of the systems showing any appreciable water solubility (**Supplementary Figures S18–S21**). Due to these complications, we carried out the cytotoxicity experiments with $[Fe_2(\textbf{L1})_3](BF_4)_4$ and $[Fe_2(\textbf{L2})_3](BF_4)_4$ dissolved in DMSO and

these solutions were then diluted with biological media to the required concentrations.

Due to the modest water solubility of many drug candidates, it is common to use DMSO to solubilize compounds for cytotoxicity experiments. However, it is also well known that DMSO can displace coordinated ligands and decompose metal complexes (Patra et al., 2013; Vellas et al., 2013; Hall et al., 2014; Huang et al., 2017). Therefore, the stability of the helicates in neat DMSO and a 1:19 v/v DMSO:water mixture was examined before carrying out the cytotoxicity experiments. The stabilities of $[Fe_2(\textbf{L1})_3](BF_4)_4$ and $[Fe_2(\textbf{L2})_3](BF_4)_4$ in these solvents were monitored using ^{1}H NMR and UV-vis spectroscopy (**Supplementary Figures S14, S15**). Both complexes completely decomposed (*ca.* 3 h for $[Fe_2(\textbf{L1})_3](BF_4)_4$ and 24 h for $[Fe_2(\textbf{L2})_3](BF_4)_4$) in neat DMSO liberating the free ligands and presumably forming $[Fe(DMSO)_6]^{2+}$ (White et al., 2007).

The helicates were more long lived in 1:19 v/v DMSO:water mixtures. A 72 h UV-visible stability study of $[Fe_2(\textbf{L1})_3](BF_4)_4$ and $[Fe_2(\textbf{L2})_3](BF_4)_4$ in 1:19 v/v DMSO:water was conducted to replicate the timeframe of the biological testing (**Supplementary Figures S16, S17**). Interestingly, the smaller $[Fe_2(\textbf{L1})_3](BF_4)_4$ showed no signs of decomposition (within the uncertainty of the measurement) whereas the larger $[Fe_2(\textbf{L2})_3](BF_4)_4$ did slowly degrade, approximately 43% of the $[Fe_2(\textbf{L2})_3](BF_4)_4$ was still present in solution after 72 h. Given the moderate to good stability of the helicates under conditions similar to those required for the cytotoxicity assay we proceeded to measure the *in vitro* antiproliferative activity of the compounds.

The ligands (**L1** and **L2**) and helicates $[Fe_2(\textbf{L1})_3](BF_4)_4$ and $[Fe_2(\textbf{L2})_3](BF_4)_4$ were subjected to the sulforhodamine B cytotoxicity assay in the human cancer cell lines HCT116 (colorectal carcinoma), NCI-H460 (non-small cell lung carcinoma), SiHa (cervical carcinoma), and SW480 (colon adenocarcinoma) (**Table 1**). **L1** and **L2** proved to be insoluble under the conditions of the experiments, and therefore their antiproliferative activity could not be determined (**Table 1**). The helicates $[Fe_2(\textbf{L1})_3](BF_4)_4$ and $[Fe_2(\textbf{L2})_3](BF_4)_4$ were both active *in vitro* against all the cancer cells tested. The smaller $[Fe_2(\textbf{L1})_3](BF_4)_4$ was more active than $[Fe_2(\textbf{L2})_3](BF_4)_4$ against all the cell lines examined, and displayed low μM activity against HCT116 ($IC_{50} = 7.1 \pm 0.5\ \mu M$) and NCI-H460 ($IC_{50} = 4.9 \pm 0.4\ \mu M$) cancer cells. Unfortunately, direct comparisons with the previously studied isostructural helicates $[Fe_2(\textbf{L}_{\textbf{Pyim}})_3]^{4+}$ and $[Fe(\textbf{L}_{\textbf{pyimR}})_3]^{2+}$ are difficult as their cytotoxicity was

TABLE 1 | IC_{50} values (μM) for **L1** and **L2** and the iron(II) cylinders against HCT116 (human colorectal carcinoma), NCI-H460 (human non-small cell lung carcinoma), SiHa (human cervical carcinoma), and SW480 (human colon adenocarcinoma) cancer cells as compared to cisplatin, expressed as mean ± standard error ($n = 3$, incubation period 72 h).

Compound	IC_{50}/μM			
	HCT116	NCI-H460	SiHa	SW480
L1	n.d.	n.d.	n.d.	n.d.
L2	n.d.	n.d.	n.d.	n.d.
rac-[Fe₂(**L1**)₃](BF₄)₄	7.1 ± 0.5	4.9 ± 0.4	39 ± 2	24 ± 4
rac/meso-[Fe₂(**L2**)₃](BF₄)₄	19 ± 1	46 ± 15	55 ± 15	13 ± 4
L_pyim Steel et al. (2021a)	21 ± 6	31 ± 4	42 ± 3	46 ± 5
rac-[Fe₂(**L_Pyim**)₃](BF₄)₄	9 ± 2	10 ± 3	26 ± 4	28 ± 7
[(Rh(Cp*)Cl)₂(**L_pyim**)] Steel et al. (2021a)	78 ± 21	>100	45 ± 4	73 ± 5
[Fe(H₂O)₆](BF₄)₂	>200	184 ± 11	>500	>300
Cisplatin Tremlett et al. (2019)	2.5 ± 0.3	0.80 ± 0.03	3.0 ± 0.6	8.1 ± 2.9

n.d., not determined due to the poor solubility of the compound.

determined with different cell lines. However, the low μM activity observed for [Fe₂(**L1**)₃](BF₄)₄ suggests that it could be more active than the [Fe₂(**L_Pyim**)₃]⁴⁺ helicates (IC_{50} values ranged from 19–52 μM, despite having been determined in different cell lines) (Hotze et al., 2008). The observed activity of [Fe₂(**L1**)₃](BF₄)₄ is similar in magnitude to that found by Scott et al. for their family of [Fe₂(**L_pyimR**)₃]²⁺ helicates (Song et al., 2021). However, the [Fe₂(**L_pyimR**)₃]²⁺ systems are more effective overall with some of that family displaying nanomolar activities (Kaner et al., 2016; Song et al., 2020). We have recently studied the cytotoxicity of a small family of dimetallic organometallic (Ru, Rh, Os, and Ir) complexes (Steel et al., 2021a) of **L_Pyim** against the same series of cell lines enabling a more direct comparison (**Table 1**). Both helicates displayed better activity than the dimetallic complexes and **L_Pyim** across the range of cell lines. Presumably the higher activity of the helicates is associated with the different molecular shape and higher charge. While the *in vitro* activity of the [Fe₂(**L1**)₃](BF₄)₄ helicate is promising we note that the widely used anti-cancer drug cisplatin is more active in all the cell lines examined (**Table 1**). However, the mode of action of this covalent DNA binder, in comparison to supramolecular structures that are more likely to form non-covalent interactions with biological targets, will be very different, making any direct comparison difficult.

CONCLUSION

Two new di(2,2′-bipyridine) ligands, 2,6-bis([2,2′-bipyridin]-5-ylethynyl)-pyridine (**L1**) and bis(4-([2,2′-bipyridin]-5-ylethynyl)-phenyl)methane (**L2**) were synthesized and exploited to generate two triple-stranded metallo-cylinders, [Fe₂(**L1**)₃](BF₄)₄ and [Fe₂(**L2**)₃](BF₄)₄. The ligands and cylinders were characterized by elemental analysis, ESIMS and UV-vis, ¹H−, ¹³C−, and DOSY-NMR spectroscopies. The molecular structures of the [Fe₂**L**₃](BF₄)₄ cylinders were confirmed using X-ray crystallography. Both [Fe₂(**L1**)₃](BF₄)₄ and [Fe₂(**L2**)₃](BF₄)₄ crystallized as racemic (*rac*) mixtures of the ΔΔ (P) and ΛΛ (M) helicates. NMR spectroscopy and ESIMS confirmed the presence of the [Fe₂**L**₃]⁴⁺ supramolecular architectures in solution. However, ¹H NMR spectra showed that in solution the larger [Fe₂(**L2**)₃](BF₄)₄ was present as a mixture of the *rac*-ΔΔ/ΛΛ and *meso*-ΔΛ isomers. The host-guest chemistry of the helicates, which both feature an accessible central cavity, was examined with several small drug molecules, including cisplatin and 5-fluorouracil. However, none of the potential guests were found to bind within the helicates, despite molecular modelling confirming that there were no obvious steric impediments to the interaction. Cytotoxicity assays demonstrated that both helicates were active against the four cell lines examined. The smaller *rac*-[Fe₂(**L1**)₃](BF₄)₄ helicate was more cytotoxic than the larger *rac/meso*-[Fe₂(**L2**)₃](BF₄)₄ analogue and displayed promising low μM antiproliferative activity against HCT116 (IC_{50} = 7.1 ± 0.5 μM) and NCI-H460 (IC_{50} = 4.9 ± 0.4 μM) human cancer cells. Although both helicates were less active than the widely used anti-cancer drug cisplatin, these results suggest that helicates constructed from di(2,2′-bipyridine) ligands have potential as anti-cancer agents in their own right. The combination of a cytotoxic supramolecular structure with encapsulated drugs may result in synergistic activity. However, the poor aqueous solubility and modest stability in biological media of the current [Fe₂(**L1**)₃](BF₄)₄ helicates means that the properties of these compounds will need to be fine-tuned to overcome these shortfalls. This could potentially be achieved by using more kinetically inert metal ions such as Ru(II) (Glasson et al., 2008; Kumar et al., 2015) or Co(III) (Symmers et al., 2015; Burke et al., 2018; Crlikova et al., 2020) to assemble the helicates.

DATA AVAILABILITY STATEMENT

The original contributions presented in the study are included in the article/**Supplementary Material**, further inquiries can be directed to the corresponding author.

AUTHOR CONTRIBUTIONS

LL, JC, CH, and LW conceived the idea. JC, CH, and LW obtained the funding. LL and JC analyzed the data and wrote the manuscript. LL conducted the synthesis. RV collected and refined the X-ray data. MR conducted cytotoxicity studies and

SUPPLEMENTARY MATERIAL

The Supplementary Material for this article can be found online at: https://www.frontiersin.org/articles/10.3389/fchem.2021.697684/full#supplementary-material

REFERENCES

Ahmedova, A., Mihaylova, R., Momekova, D., Shestakova, P., Stoykova, S., Zaharieva, J., et al. (2016a). M₂L₄ Coordination Capsules With Tunable Anticancer Activity Upon Guest Encapsulation. *Dalton Trans.* 45, 13214–13221. doi:10.1039/c6dt01801g

Ahmedova, A., Mihaylova, R., Stoykova, S., Mihaylova, V., Paunova-Krasteva, T., Mihaylov, L., et al. (2020). Enhanced Cellular Uptake of Platinum by a Tetracationic Pt(II) Nanocapsule and its Implications to Cancer Treatment. *Eur. J. Pharm. Sci.* 155, 105545. doi:10.1016/j.ejps.2020.105545

Ahmedova, A., Momekova, D., Yamashina, M., Shestakova, P., Momekov, G., Akita, M., et al. (2016b). Anticancer Potencies of PtII - and PdII -Linked M₂L₄ Coordination Capsules With Improved Selectivity. *Chem. Asian J.* 11, 474–477. doi:10.1002/asia.201501238

Albrecht, M. (2001). "Let's Twist Again" Double-Stranded, Triple-Stranded, and Circular Helicates. *Chem. Rev.* 101, 3457–3498. doi:10.1021/cr0103672

Albrecht, M. (2020). Catecholate-Based Helicates. *Eur. J. Inorg. Chem.* 2020, 2227–2237. doi:10.1002/ejic.202000255

Albrecht, M., Chen, X., and Van Craen, D. (2019). From Hierarchical Helicates to Functional Supramolecular Devices. *Chem. Eur. J.* 25, 4265–4273. doi:10.1002/chem.201804963

Allison, S. J., Cooke, D., Davidson, F. S., Elliott, P. I. P., Faulkner, R. A., Griffiths, H. B. S., et al. (2018). Ruthenium-Containing Linear Helicates and Mesocates With Tuneable P53-Selective Cytotoxicity in Colorectal Cancer Cells. *Angew. Chem. Int. Ed.* 57, 9799–9804. doi:10.1002/anie.201805510

Anthony, E. J., Bolitho, E. M., Bridgewater, H. E., Carter, O. W. L., Donnelly, J. M., Imberti, C., et al. (2020). Metallodrugs Are Unique: Opportunities and Challenges of Discovery and Development. *Chem. Sci.* 11, 12888–12917. doi:10.1039/d0sc04082g

August, D. P., Nichol, G. S., and Lusby, P. J. (2016). Maximizing Coordination Capsule-Guest Polar Interactions in Apolar Solvents Reveals Significant Binding. *Angew. Chem. Int. Ed.* 55, 15022–15026. doi:10.1002/anie.201608229

Austin, W. B., Bilow, N., Kelleghan, W. J., and Lau, K. S. Y. (1981). Facile Synthesis of Ethynylated Benzoic Acid Derivatives and Aromatic Compounds via Ethynyltrimethylsilane. *J. Org. Chem.* 46, 2280–2286. doi:10.1021/jo00324a015

Bardhan, D., and Chand, D. K. (2019). Palladium(II)-Based Self-Assembled Heteroleptic Coordination Architectures: A Growing Family. *Chem. Eur. J.* 25, 12241–12269. doi:10.1002/chem.201900831

Boiocchi, M., and Fabbrizzi, L. (2014). Double-stranded Dimetallic Helicates: Assembling-Disassembling Driven by the Cu(I)/Cu(II) Redox Change and the Principle of Homochiral Recognition. *Chem. Soc. Rev.* 43, 1835–1847. doi:10.1039/c3cs60428d

Boros, E., Dyson, P. J., and Gasser, G. (2020). Classification of Metal-Based Drugs According to Their Mechanisms of Action. *Chem.* 6, 41–60. doi:10.1016/j.chempr.2019.10.013

Brabec, V., Howson, S. E., Kaner, R. A., Lord, R. M., Malina, J., Phillips, R. M., et al. (2013). Metallohelices with Activity Against Cisplatin-Resistant Cancer Cells; Does the Mechanism Involve DNA Binding? *Chem. Sci.* 4, 4407–4416. doi:10.1039/c3sc51731d

Burke, B. P., Grantham, W., Burke, M. J., Nichol, G. S., Roberts, D., Renard, I., et al. (2018). Visualizing Kinetically Robust Co(III)₄L₆ Assemblies in Vivo: SPECT Imaging of the Encapsulated [99mTc]TcO₄-Anion. *J. Am. Chem. Soc.* 140, 16877–16881. doi:10.1021/jacs.8b09582

Cardo, L., Nawroth, I., Cail, P. J., Mckeating, J. A., and Hannon, M. J. (2018). Metallo Supramolecular Cylinders Inhibit HIV-1 TARTAT Complex Formation and Viral Replication in Cellulo. *Sci. Rep.* 8, 13342. doi:10.1038/s41598-018-31513-3

Cardo, L., Sadovnikova, V., Phongtongpasuk, S., Hodges, N. J., and Hannon, M. J. (2011). Arginine Conjugates of Metallo-Supramolecular Cylinders Prescribe Helicity and Enhance DNA Junction Binding and Cellular Activity. *Chem. Commun.* 47, 6575–6577. doi:10.1039/c1cc11356a

Cerasino, L., Hannon, M. J., and Sletten, E. (2007). DNA Three-Way Junction With a Dinuclear Iron(II) Supramolecular Helicate at the Center: A NMR Structural Study. *Inorg. Chem.* 46, 6245–6251. doi:10.1021/ic062415c

Childs, L. J., Malina, J., Rolfsnes, B. E., Pascu, M., Prieto, M. J., Broome, M. J., et al. (2006). A DNA-Binding Copper(I) Metallosupramolecular cylinder that Acts as an Artificial Nuclease. *Chem. Eur. J.* 12, 4919–4927. doi:10.1002/chem.200600060

Cook, T. R., and Stang, P. J. (2015). Recent Developments in the Preparation and Chemistry of Metallacycles and Metallacages via Coordination. *Chem. Rev.* 115, 7001–7045. doi:10.1021/cr5005666

Cook, T. R., Vajpayee, V., Lee, M. H., Stang, P. J., and Chi, K.-W. (2013). Biomedical and Biochemical Applications of Self-Assembled Metallacycles and Metallacages. *Acc. Chem. Res.* 46, 2464–2474. doi:10.1021/ar400010v

Crlikova, H., Malina, J., Novohradsky, V., Kostrhunova, H., Vasdev, R. A. S., Crowley, J. D., et al. (2020). Antiproliferative Activity and Associated DNA Interactions of [Co₂L₃]⁶⁺ Cylinders Derived From Bis(bidentate) 2-Pyridyl-1,2,3-Triazole Ligands. *Organometallics* 39, 1448–1455. doi:10.1021/acs.organomet.0c00146

Cui, F., Li, S., Jia, C., Mathieson, J. S., Cronin, L., Yang, X.-J., et al. (2012). Anion-Dependent Formation of Helicates Versus Mesocates of Triple-Stranded M₂L₃ (M = Fe²⁺, Cu²⁺) Complexes. *Inorg. Chem.* 51, 179–187. doi:10.1021/ic201417y

Faulkner, A. D., Kaner, R. A., Abdallah, Q. M. A., Clarkson, G., Fox, D. J., Gurnani, P., et al. (2014). Asymmetric Triplex Metallohelices With High and Selective Activity Against Cancer Cells. *Nat. Chem.* 6, 797–803. doi:10.1038/nchem.2024

Fazio, E., Haynes, C. J. E., De La Torre, G., Nitschke, J. R., and Torres, T. (2018). A Giant M₂L₃ Metallo-Organic Helicate Based on Phthalocyanines as a Host for Electroactive Molecules. *Chem. Commun.* 54, 2651–2654. doi:10.1039/c7cc09528g

Frei, A. (2020). Metal Complexes, an Untapped Source of Antibiotic Potential? *Antibiotics* 9, 90. doi:10.3390/antibiotics9020090

Frei, A., Zuegg, J., Elliott, A. G., Baker, M., Braese, S., Brown, C., et al. (2020). Metal Complexes as a Promising Source for New Antibiotics. *Chem. Sci.* 11, 2627–2639. doi:10.1039/c9sc06460e

Gamba, I., Rama, G., Ortega-Carrasco, E., Maréchal, J.-D., Martínez-Costas, J., Eugenio Vázquez, M., et al. (2014). Programmed Stereoselective Assembly of DNA-Binding Helical Metallopeptides. *Chem. Commun.* 50, 11097–11100. doi:10.1039/c4cc03606a

Gao, W.-X., Zhang, H.-N., and Jin, G.-X. (2019). Supramolecular Catalysis Based on Discrete Heterometallic Coordination-Driven Metallacycles and Metallacages. *Coord. Chem. Rev.* 386, 69–84. doi:10.1016/j.ccr.2019.01.023

Glasson, C. R. K., Meehan, G. V., Clegg, J. K., Lindoy, L. F., Smith, J. A., Keene, F. R., et al. (2008). Microwave Synthesis of a Rare [Ru₂L₃]⁴⁺ Triple Helicate and its Interaction With DNA. *Chem. Eur. J.* 14, 10535–10538. doi:10.1002/chem.200801790

Glasson, C. R. K., Meehan, G. V., Motti, C. A., Clegg, J. K., Turner, P., Jensen, P., et al. (2011a). New Nickel(II) and Iron(II) Helicates and Tetrahedra Derived From Expanded Quaterpyridines. *Dalton Trans.* 40, 10481–10490. doi:10.1039/c1dt10667h

Glasson, C. R. K., Meehan, G. V., Motti, C. A., Clegg, J. K., Turner, P., Jensen, P., et al. (2011b). Nickel(II) and Iron(II) Triple Helicates Assembled from Expanded Quaterpyridines Incorporating Flexible Linkages. *Dalton Trans.* 40, 12153–12159. doi:10.1039/c1dt10820d

Goetz, S., and Kruger, P. E. (2006). A New Twist in Anion Binding: Metallo-Helicate Hosts for Anionic Guests. *Dalton Trans.*, 1277–1284. doi:10.1039/b514580e

Gómez-González, J., Pérez, Y., Sciortino, G., Roldan-Martín, L., Martínez-Costas, J., Maréchal, J. D., et al. (2021). Dynamic Stereoselection of Peptide Helicates and Their Selective Labeling of DNA Replication Foci in Cells*. *Angew. Chem. Int. Ed. Engl.* 60, 8859–8866. doi:10.1002/anie.202013039

Gómez-González, J., Peña, D. G., Barka, G., Sciortino, G., Maréchal, J.-D., Vázquez López, M., et al. (2018). Directed Self-Assembly of Trimeric DNA-Bindingchiral Miniprotein Helicates. *Front. Chem.* 6, 520. doi:10.3389/fchem.2018.00520

Grosshenny, V., Romero, F. M., and Ziessel, R. (1997). Construction of Preorganized Polytopic Ligands via Palladium-Promoted Cross-Coupling Reactions. *J. Org. Chem.* 62, 1491–1500. doi:10.1021/jo962068w

Hall, M. D., Telma, K. A., Chang, K.-E., Lee, T. D., Madigan, J. P., Lloyd, J. R., et al. (2014). Say No to DMSO: Dimethylsulfoxide Inactivates Cisplatin, Carboplatin, and Other Platinum Complexes. *Cancer Res.* 74, 3913–3922. doi:10.1158/0008-5472.can-14-0247

Hannon, M. J., and Childs, L. J. (2004). Helices and Helicates: Beautiful Supramolecular Motifs With Emerging Applications. *Supramolecular Chem.* 16, 7–22. doi:10.1080/10610270310001632386

Hannon, M. J., Meistermann, I., Isaac, C. J., Blomme, C., Rodger, A., and Aldrich-Wright, J. R. (2001a). Paper: a Cheap yet Effective Chiral Stationary Phase for Chromatographic Resolution of Metallo-Supramolecular Helicates. *Chem. Commun.*, 1078–1079. doi:10.1039/b101970h

Hannon, M. J., Moreno, V., Prieto, M. J., Moldrheim, E., Sletten, E., Meistermann, I., et al. (2001b). Intramolecular DNA Coiling Mediated by a Metallo-Supramolecular Cylinder. *Angew. Chem. Int. Ed.* 40, 880–884. doi:10.1002/1521-3773(20010302)40:5<879::aid-anie879>3.0.co;2-x

Hannon, M. J., Painting, C. L., Jackson, A., Hamblin, J., and Errington, W. (1997). An Inexpensive Approach to Supramolecular Architecture. *Chem. Commun.*, 1807–1808. doi:10.1039/a703713i

Hartinger, C. G., and Dyson, P. J. (2009). Bioorganometallic Chemistry-From Teaching Paradigms to Medicinal Applications. *Chem. Soc. Rev.* 38, 391–401. doi:10.1039/b707077m

Holtze, A. C. G., Kariuki, B. M., and Hannon, M. J. (2006). Dinuclear Double-Stranded Metallosupramolecular Ruthenium Complexes: Potential Anticancer Drugs. *Angew. Chem. Int. Ed.* 45, 4839–4842. doi:10.1002/anie.200601351

Hong, C. M., Bergman, R. G., Raymond, K. N., and Toste, F. D. (2018). Self-Assembled Tetrahedral Hosts as Supramolecular Catalysts. *Acc. Chem. Res.* 51, 2447–2455. doi:10.1021/acs.accounts.8b00328

Hotze, A. C. G., Hodges, N. J., Hayden, R. E., Sanchez-Cano, C., Paines, C., Male, N., et al. (2008). Supramolecular Iron Cylinder with Unprecedented DNA Binding Is a Potent Cytostatic and Apoptotic Agent without Exhibiting Genotoxicity. *Chem. Biol.* 15, 1258–1267. doi:10.1016/j.chembiol.2008.04.016

Howson, S. E., Allan, L. E. N., Chmel, N. P., Clarkson, G. J., Van Gorkum, R., and Scott, P. (2009). Self-assembling Optically Pure Fe(A-B)₃ Chelates. *Chem. Commun.*, 1727–1729. doi:10.1039/b821573a

Howson, S. E., Bolhuis, A., Brabec, V., Clarkson, G. J., Malina, J., Rodger, A., et al. (2012). Optically Pure, Water-Stable Metallo-Helical "flexicate" Assemblies with Antibiotic Activity. *Nat. Chem* 4, 31–36. doi:10.1038/nchem.1206

Howson, S. E., and Scott, P. (2011). Approaches to the Synthesis of Optically Pure Helicates. *Dalton Trans.* 40, 10268–10277. doi:10.1039/c1dt11423a

Hrabina, O., Malina, J., Scott, P., and Brabec, V. (2020). Cationic Fe(II) Triplex-Forming Metallohelices as DNA Bulge Binders. *Chem. Eur. J.* 26, 16554–16562. doi:10.1002/chem.202004060

Huang, H., Humbert, N., Bizet, V., Patra, M., Chao, H., Mazet, C., et al. (2017). Influence of the Dissolution Solvent on the Cytotoxicity of Octahedral Cationic Ir(III) Hydride Complexes. *J. Organomet. Chem.* 839, 15–18. doi:10.1016/j.jorganchem.2016.12.010

Jiang, P., Wu, W.-Y., Tang, T.-H., Chen, Z.-F., Fang, Y.-C., and Wan, R. (2019). ¹H NMR STUDY OF THE HOST-GUEST CHEMISTRY IN A SUPRAMOLECULAR HELICATE FE(II)₂L₃ SOLUTION. *Quim. Nova* 42, 412–417. doi:10.21577/0100-4042.20170355

Kaner, R. A., Allison, S. J., Faulkner, A. D., Phillips, R. M., Roper, D. I., Shepherd, S. L., et al. (2016). Anticancer Metallohelices: Nanomolar Potency and High Selectivity. *Chem. Sci.* 7, 951–958. doi:10.1039/c5sc03677a

Kaner, R. A., and Scott, P. (2015). Metallohelices: Potential Mimetics of α-Helical Peptides in Cancer Treatment? *Future Med. Chem.* 7, 1–4. doi:10.4155/fmc.14.150

Kumar, S. V., Lo, W. K. C., Brooks, H. J. L., and Crowley, J. D. (2015). Synthesis, Structure, Stability and Antimicrobial Activity of a Ruthenium(II) Helicate Derived from a Bis-Bidentate "click" Pyridyl-1,2,3-Triazole Ligand. *Inorg. Chim. Acta* 425, 1–6. doi:10.1016/j.ica.2014.10.011

Lehn, J. M., Rigault, A., Siegel, J., Harrowfield, J., Chevrier, B., and Moras, D. (1987). Spontaneous Assembly of Double-Stranded Helicates from Oligobipyridine Ligands and Copper(I) Cations: Structure of an Inorganic Double helix. *Proc. Natl. Acad. Sci.* 84, 2565–2569. doi:10.1073/pnas.84.9.2565

Li, M., Howson, S. E., Dong, K., Gao, N., Ren, J., Scott, P., et al. (2014). Chiral Metallohelical Complexes Enantioselectively Target Amyloid β for Treating Alzheimer's Disease. *J. Am. Chem. Soc.* 136, 11655–11663. doi:10.1021/ja502789e

Li, M., Zhao, C., Ren, J., and Qu, X. (2015). Chiral Metallo-Supramolecular Complex Directed Enantioselective Self-Assembly of β-Sheet Breaker Peptide for Amyloid Inhibition. *Small* 11, 4651–4655. doi:10.1002/smll.201501329

Malina, J., Hannon, M. J., and Brabec, V. (2008). DNA Binding of Dinuclear Iron(II) Metallosupramolecular Cylinders. DNA Unwinding and Sequence Preference. *Nucleic Acids Res.* 36, 3630–3638. doi:10.1093/nar/gkn244

Malina, J., Hannon, M. J., and Brabec, V. (2016). Iron(II) Supramolecular Helicates Interfere with the HIV-1 Tat-TAR RNA Interaction Critical for Viral Replication. *Sci. Rep.* 6, 29674. doi:10.1038/srep29674

Malina, J., Hannon, M. J., and Brabec, V. (2014). Recognition of DNA Bulges by Dinuclear Iron(II) Metallosupramolecular Helicates. *FEBS J.* 281, 987–997. doi:10.1111/febs.12696

Malina, J., Hannon, M. J., and Brabec, V. (2007). Recognition of DNA Three-Way Junctions by Metallosupramolecular Cylinders: Gel Electrophoresis Studies. *Chem. Eur. J.* 13, 3871–3877. doi:10.1002/chem.200700159

Malina, J., Scott, P., and Brabec, V. (2015a). Recognition of DNA/RNA Bulges by Antimicrobial and Antitumor Metallohelices. *Dalton Trans.* 44, 14656–14665. doi:10.1039/c5dt02018b

Malina, J., Scott, P., and Brabec, V. (2015b). Shape-selective Recognition of DNA Abasic Sites by Metallohelices: Inhibition of Human AP Endonuclease 1. *Nucleic Acids Res.* 43, 5297–5306. doi:10.1093/nar/gkv438

McNeill, S. M., Giles, N. M., Preston, D., Jones, P. P., Crowley, J. D., and Giles, G. I. (2020). Quadruply Stranded Metallo-Supramolecular Helicate [Pd₂(hextrz)₄]⁴⁺ Acts as a Molecular Mimic of Cytolytic Peptides. *Chem. Res. Toxicol.* 33, 1822–1834. doi:10.1021/acs.chemrestox.0c00061

McNeill, S. M., Preston, D., Lewis, J. E. M., Robert, A., Knerr-Rupp, K., Graham, D. O., et al. (2015). Biologically Active [Pd₂L₄]⁴⁺ Quadruply-Stranded Helicates: Stability and Cytotoxicity. *Dalton Trans.* 44, 11129–11136. doi:10.1039/c5dt01259g

Mjos, K. D., and Orvig, C. (2014). Metallodrugs in Medicinal Inorganic Chemistry. *Chem. Rev.* 114, 4540–4563. doi:10.1021/cr400460s

Moldrheim, E., Hannon, M. J., Meistermann, I., Rodger, A., and Sletten, E. (2002). Interaction between a DNA Oligonucleotide and a Dinuclear Iron(II) Supramolecular Cylinder; an NMR and Molecular Dynamics Study. *J. Biol. Inorg. Chem.* 7, 770–780. doi:10.1007/s00775-002-0354-2

Oleksi, A., Blanco, A. G., Boer, R., Usón, I., Aymamí, J., Rodger, A., et al. (2006). Molecular Recognition of a Three-Way DNA Junction by a Metallosupramolecular Helicate. *Angew. Chem. Int. Ed.* 45, 1227–1231. doi:10.1002/anie.200503822

Paneerselvam, A. P., Mishra, S. S., and Chand, D. K. (2018). Linear and Circular Helicates: A Brief Review. *J. Chem. Sci.* 130, 96. doi:10.1007/s12039-018-1497-1

Patra, M., Joshi, T., Pierroz, V., Ingram, K., Kaiser, M., Ferrari, S., et al. (2013). DMSO-Mediated Ligand Dissociation: Renaissance for Biological Activity of N-Heterocyclic-[Ru(η⁶-arene)Cl₂] Drug Candidates. *Chem. Eur. J.* 19, 14768–14772. doi:10.1002/chem.201303341

Percástegui, E. G., Ronson, T. K., and Nitschke, J. R. (2020). Design and Applications of Water-Soluble Coordination Cages. *Chem. Rev.* 120, 13480–13544. doi:10.1021/acs.chemrev.0c00672

Phongtongpasuk, S., Paulus, S., Schnabl, J., Sigel, R. K. O., Spingler, B., Hannon, M. J., et al. (2013). Binding of a Designed Anti-cancer Drug to the Central Cavity of an RNA Three-Way Junction. *Angew. Chem. Int. Ed.* 52, 11513–11516. doi:10.1002/anie.201305079

Piguet, C., Bernardinelli, G., and Hopfgartner, G. (1997). Helicates as Versatile Supramolecular Complexes. *Chem. Rev.* 97, 2005–2062. doi:10.1021/cr960053s

Pöthig, A., and Casini, A. (2019). Recent Developments of Supramolecular Metal-Based Structures for Applications in Cancer Therapy and Imaging. *Theranostics* 9, 3150–3169. doi:10.7150/thno.31828

Richards, A. D., Rodger, A., Hannon, M. J., and Bolhuis, A. (2009). Antimicrobial Activity of an Iron Triple Helicate. *Int. J. Antimicrob. Agents* 33, 469–472. doi:10.1016/j.ijantimicag.2008.10.031

Rizzuto, F. J., Von Krbek, L. K. S., and Nitschke, J. R. (2019). Strategies for Binding Multiple Guests in Metal-Organic Cages. *Nat. Rev. Chem.* 3, 204–222. doi:10.1038/s41570-019-0085-3

Saha, S., Regeni, I., and Clever, G. H. (2018). Structure Relationships between Bis-Monodentate Ligands and Coordination Driven Self-Assemblies. *Coord. Chem. Rev.* 374, 1–14. doi:10.1016/j.ccr.2018.06.010

Samanta, S. K., and Isaacs, L. (2020). Biomedical Applications of Metal Organic Polygons and Polyhedra (MOPs). *Coord. Chem. Rev.* 410, 213181. doi:10.1016/j.ccr.2020.213181

Schmidt, A., Molano, V., Hollering, M., Pöthig, A., Casini, A., and Kühn, F. E. (2016). Evaluation of New Palladium Cages as Potential Delivery Systems for the Anticancer Drug Cisplatin. *Chem. Eur. J.* 22, 2253–2256. doi:10.1002/chem.201504930

Schoentjes, B., and Lehn, J.-M. (1995). Interaction of Double-Helical Polynuclear Copper(I) Complexes with Double-Stranded DNA. *Helv. Chim. Acta* 78, 1–12. doi:10.1002/hlca.19950780103

Sepehrpour, H., Fu, W., Sun, Y., and Stang, P. J. (2019). Biomedically Relevant Self-Assembled Metallacycles and Metallacages. *J. Am. Chem. Soc.* 141, 14005–14020. doi:10.1021/jacs.9b06222

Simpson, D. H., Hapeshi, A., Rogers, N. J., Brabec, V., Clarkson, G. J., Fox, D. J., et al. (2019). Metallohelices that Kill Gram-Negative Pathogens Using Intracellular Antimicrobial Peptide Pathways. *Chem. Sci.* 10, 9708–9720. doi:10.1039/c9sc03532j

Song, H., Postings, M., Scott, P., and Rogers, N. J. (2021). Metallohelices Emulate the Properties of Short Cationic α-helical Peptides. *Chem. Sci.* 12, 1620–1631. doi:10.1039/d0sc06412b

Song, H., Rogers, N. J., Allison, S. J., Brabec, V., Bridgewater, H., Kostrhunova, H., et al. (2019). Discovery of Selective, Antimetastatic and Anti-cancer Stem Cell Metallohelicesviapost-Assembly Modification. *Chem. Sci.* 10, 8547–8557. doi:10.1039/c9sc02651g

Song, H., Rogers, N. J., Brabec, V., Clarkson, G. J., Coverdale, J. P. C., Kostrhunova, H., et al. (2020). Triazole-based, Optically-Pure Metallosupramolecules; Highly Potent and Selective Anticancer Compounds. *Chem. Commun.* 56, 6392–6395. doi:10.1039/d0cc02429e

Steel, T. R., Tong, K. K. H., Söhnel, T., Jamieson, S. M. F., Wright, L. J., Crowley, J. D., et al. (2021a). Homodinuclear Organometallics of Ditopic N,N-chelates: Synthesis, Reactivity and *In Vitro* Anticancer Activity. *Inorg. Chim. Acta* 518, 120220. doi:10.1016/j.ica.2020.120220

Steel, T. R., Walsh, F., Wieczorek-Błauż, A., Hanif, M., and Hartinger, C. G. (2021b). Monodentately-coordinated Bioactive Moieties in Multimodal Half-

sandwich Organoruthenium Anticancer Agents. *Coord. Chem. Rev.* 439, 213890. doi:10.1016/j.ccr.2021.213890

Symmers, P. R., Burke, M. J., August, D. P., Thomson, P. I. T., Nichol, G. S., Warren, M. R., et al. (2015). Non-equilibrium Cobalt(iii) "click" Capsules. *Chem. Sci.* 6, 756–760. doi:10.1039/c4sc03036b

Therrien, B. (2015). Biologically Relevant Arene Ruthenium Metalla-Assemblies. *CrystEngComm* 17, 484–491. doi:10.1039/c4ce02146k

Tran, N. M., and Yoo, H. (2020). Recent Advances in Heteroleptic Multiple-Stranded Metallosupramolecules. *Dalton Trans.* 49, 11819–11827. doi:10.1039/d0dt02243h

Tremlett, W. D. J., Tong, K. K. H., Steel, T. R., Movassaghi, S., Hanif, M., Jamieson, S. M. F., et al. (2019). Hydroxyquinoline-derived Anticancer Organometallics: Introduction of Amphiphilic PTA as an Ancillary Ligand Increases Their Aqueous Solubility. *J. Inorg. Biochem.* 199, 110768. doi:10.1016/j.jinorgbio.2019.110768

Vasdev, R. A. S., Gaudin, L. F., Preston, D., Jogy, J. P., Giles, G. I., and Crowley, J. D. (2018). Anticancer Activity and Cisplatin Binding Ability of Bis-Quinoline and Bis-Isoquinoline Derived [Pd₂L₄]⁴⁺ Metallosupramolecular Cages. *Front. Chem.* 6, 563. doi:10.3389/fchem.2018.00563

Vasdev, R., Preston, D., Scottwell, S., Brooks, H., Crowley, J., and Schramm, M. (2016). Oxidatively Locked [Co₂L₃]⁶⁺ Cylinders Derived from Bis(bidentate) 2-Pyridyl-1,2,3-Triazole "Click" Ligands: Synthesis, Stability, and Antimicrobial Studies. *Molecules* 21, 1548. doi:10.3390/molecules21111548

Vellas, S., Lewis, J., Shankar, M., Sagatova, A., Tyndall, J., Monk, B., et al. (2013). [Fe₂L₃]⁴⁺ Cylinders Derived from Bis(bidentate) 2-Pyridyl-1,2,3-Triazole "Click" Ligands: Synthesis, Structures and Exploration of Biological Activity. *Molecules* 18, 6383–6407. doi:10.3390/molecules18066383

White, A. P., Robertson, K. N., Cameron, T. S., Liengme, B. V., Leznoff, D. B., Trudel, S., et al. (2007). Synthesis and Characterization of [M(DMSO)₆][SnCl₆] Complexes (M = Fe²⁺, Co²⁺, and Ni²⁺) - an Old Mystery Solved. *Can. J. Chem.* 85, 372–378. doi:10.1139/v07-042

Yang, J., Krbek, L. K. S., Yu, L., Ronson, T. K., Thoburn, J. D., Carpenter, J. P., et al. (2021). Glucose Binding Drives Reconfiguration of a Dynamic Library of Urea-Containing Metal-Organic Assemblies. *Angew. Chem. Int. Ed.* 60, 4485–4490. doi:10.1002/anie.202014568

Yoshizawa, M., Klosterman, J. K., and Fujita, M. (2009). Functional Molecular Flasks: New Properties and Reactions within Discrete, Self-Assembled Hosts. *Angew. Chem. Int. Ed.* 48, 3418–3438. doi:10.1002/anie.200805340

Yu, H., Li, M., Liu, G., Geng, J., Wang, J., Ren, J., et al. (2012). Metallosupramolecular Complex Targeting an α/β Discordant Stretch of Amyloid β Peptide. *Chem. Sci.* 3, 3145–3153. doi:10.1039/c2sc20372c

Zhao, A., Howson, S. E., Zhao, C., Ren, J., Scott, P., Wang, C., et al. (2017). Chiral Metallohelices Enantioselectively Target Hybrid Human Telomeric G-Quadruplex DNA. *Nucleic Acids Res.* 45, 5026–5035. doi:10.1093/nar/gkx244

Zhao, A., Zhao, C., Ren, J., and Qu, X. (2016). Enantioselective Targeting Left-Handed Z-G-Quadruplex. *Chem. Commun.* 52, 1365–1368. doi:10.1039/c5cc08401f

Zhao, C., Song, H., Scott, P., Zhao, A., Tateishi-Karimata, H., Sugimoto, N., et al. (2018). Mirror-Image Dependence: Targeting Enantiomeric G-Quadruplex DNA Using Triplex Metallohelices. *Angew. Chem. Int. Ed.* 57, 15723–15727. doi:10.1002/anie.201809207

Zhao, C., Wu, L., Ren, J., Xu, Y., and Qu, X. (2013). Targeting Human Telomeric Higher-Order DNA: Dimeric G-Quadruplex Units Serve as Preferred Binding Site. *J. Am. Chem. Soc.* 135, 18786–18789. doi:10.1021/ja410723r